Krzysztof KUKIEŁKA, Radosław PATYK, Leon KUKIEŁKA, Łukasz BOHDAL
Koszalin University of Technology, Mechanical Engineering Faculty
ul. Racławicka 15-17, 75-620 Koszalin, Poland
e-mail: krzysztof.kukielka@tu.koszalin.pl, radoslaw.patyk@tu.koszalin.pl, leon.kukielka@tu.koszalin.pl, lukasz.bohdal@tu.koszalin.p

STRENGTH AND FATIGUE NUMERICAL ANALYSIS OF JOINTED-TELESCOPIC POWER TAKE-OFF SHAFT

Summary

The aim of this work is to develop a numerical application to strength and fatigue numerical analysis of jointed-telescopic Power Take-Off shaft. Exemplary results for equivalent of stress in whole shaft and in a part of stress concentration are shown. Presented chart of changing of the number of the correct cycles operation of the PTO shaft depending on the torsional angle allows to predict a shaft life. From numerical analyses of process it follows that the numerically tested system can withstand the load associated with the vibration phenomena and is properly designed. Furthermore, it was found that the shaft at the maximum rotational operating speeds, is working at frequencies under resonance.
***Key words**: power take-off shaft, strength analysis, fatigue wear analysis, numerical analysis*

WYTRZYMAŁOŚCIOWA I ZMĘCZENIOWA ANALIZA NUMERYCZNA WAŁU PRZEGUBOWO-TELESKOPOWEGO

Streszczenie

Celem niniejszej pracy jest opracowanie aplikacji numerycznej do wytrzymałościowej i zmęczeniowej analizy numerycznej wału przegubowo-teleskopowego. Zamieszczono przykładowe wyniki dla naprężeń zredukowanych dla całego wałka oraz w miejscach ich koncentracji. Zaprezentowany wykres zależności liczby cykli pracy od kąta odchylenia widłaków pozwala na prognozowanie trwałości WPM. Z przeprowadzonych analiz numerycznych procesu wynika, że badany numerycznie układ wytrzymuje obciążenia związane ze zjawiskami drganiowymi i jest prawidłowo zaprojektowany. Ponadto, stwierdzono, że wał przy maksymalnych obrotowych prędkościach roboczych pracuje w częstotliwościach podrezonansowych
***Słowa kluczowe**: wał przegubowo-teleskopowy, analiza wytrzymałościowa, analiza zmęczeniowa, analiza numeryczna*

1. Introduction

Modern farm tractor on the farm isn't only a source of tractive force, but also provides the energy to drive machinery and equipment working elements aggregated with the tractor. It can be also used to drive assemblies of stationary machinery.

Jointed or jointed-telescopic Power Take-Off shaft (PTO) are used for power transmission and are most commonly used in automotive, agricultural, forestry, and construction (fig. 1). Using the relay shaft is driven attached harvesters for cereals, beet, potatoes, forage harvesters, binders, spinners, planters, etc. In order to enable the transfer of power from each tractor to any agricultural machines, splines of shafts relay and rotation speed were normalized. PTO shafts can rotate at a constant speed, dependent only on the speed of the engine crankshaft, and completely independent of the speed of the tractor or engaged gear. The rotational speed of the shaft is standardized and is it 540, 750 or 1000 ± 15 rpm at rated rotational engine speed [3, 14].

PTO shafts may also have a so called rotational synchronized speed, i.e., dependent on the speed of the tractor (the engaged gear). Variable speed shaft is proportional to the movement speed of the tractor. Speed synchronization is applicable, among others, in the case of driving a sowing instrument, where the speed of the seed is dependent from the speed of the tractor. Speed must be also synchronized in shaft transmitting power from the engine to the drive wheels of the tractor trailers and machines in order to increase the traction of the whole unit. The rotational speed of the shaft must be such that the peripheral speed of the drive wheels of the tractor and trailer or machinery with the driving axle were the same [3]. Presently the shaft with independent rotation is standard in every new tractor. From its power class and sets depends that has one speed – 540 rpm, or the ability to choose between 540 and 1000 rpm [3].

a)

b)

Source: / Źródło:

Fig. 1. View exemplary jointed-telescopic power take-off shafts to drive agricultural machinery without (a) and with overload clutch (b)
Rys. 1. Widok przykładowych wałów przegubowo-teleskopowych do napędu maszyn rolniczych bez (a) i ze sprzęgłem przeciążeniowym) (b)

Jointed-telescopic Power Take-Off shaft consists of the following components: external yoke, internal yoke, cross

connector, the spline shaft with a pipe or external or internal pipe and casing (fig. 2).

Depending on the design of PTO shafts puts the following requirements:

- working length 500-2000 mm,
- maximum speed up to 1000 rpm,
- maximum transmitted power up to 200 kM,
- maximum moment of 1400 Nm,
- the possibility of using the clutch for overload protection (fig. 1b).

It is optimal that during the field work when all the working elements of PTO shaft are working in its axis or have a small deviation angle of from the axis of the drive shaft from the tractor to driven machine. Using a PTO shaft in a different setting, e.g., when turning causes it to run-out, which contributes to its rapid wear. Examples of typical mechanical damage of jointed-telescopic Power Take-Off shafts, caused by improper use are shown on figure 3.

One of the fundamental problems associated with the operation of PTO shafts is to determine:

- states of stress in structural elements and areas of its accumulation, depending on the angle of deviation driving shaft and driven shaft,
- shaft fatigue wear at different deviation angles,
- frequencies periodicity of the shaft and the increase in stress- induced by increase in the frequency force.

In order to perform these calculations and determine acceptable working conditions PTO shaft, due to specified criteria and constraints of limitations, developed applications on the computer system ANSYS. Applications allow, among other things, to carry out of the strength and fatigue numerical analysis and to determine the impact of the degree of twisting of external yoke operational strength.

Source: / Źródło:

Fig. 2. View of the most important parts of the Jointed-telescopic Power Take-Off shaft
Rys. 2. Widok najważniejszych elementów wałka przegubowo-teleskopowego

Source: / Źródło:

Fig. 3. Typical mechanical damage of jointed-telescopic Power Take-Off shaft: a – crack of internal pipe, b, c, d – fatigue wear of external yoke, bended yoke, bearing damage and broke out of cross connector, e – fatigue wear of internal yoke
Rys. 3. Typowe uszkodzenia wałka przegubowo-teleskopowego: a – pęknięcie rury wewnętrznej, b, c, d – zużycie zmęczeniowe widłaka zewnętrznego, rozgięcie widłaka, uszkodzenie łożyskowania i wyrwanie krzyżaka, e – zużycie zmęczeniowe widłaka wewnętrznego

2. Strength and fatigue analysis of PTO shaft

2.1. Application for analysis of physical phenomena

The first step in the development of applications for strength analysis is to develop a solid model PTO shaft. To create geometry PTO SolidWorks software was used (fig. 4).

On the other hand calculations were performed in ANSYS. In the computer model assumes that, the shaft is made of material elastic/visco-plastic (E/VP) corresponding to the parameters of steel 1.2842 [1, 2, 5, 9, 10, 11, 13]. The effects of surface roughness, the effect of thermal phenomena and the effect of friction in the fasten were missed. Geometric model was discretized to the 105025 finite elements (186617 nodes). One of external yoke has been fixed (FIXED SUPORT – fig. 5), and the second external yoke was applied moment $M_0 = 750$ [Nm]. Numerical investigations were performed for the following angles between the axis of the external and internal yoke: α = 0, 15, 30, 45, 60, 75 and 90°.

Source: / Źródło:

Fig. 5. Jointed-telescopic shaft with: a) – initial and boundary conditions, b) – discretized FEM model; number of finite elements – 105025 and nodes – 186617

Rys. 5. Wałek przegubowo-teleskopowy: a) – warunki brzegowo-początkowe, b) – model dyskretny MES; liczba węzłów – 186617, liczba elementów skończonych – 105025

2.2. Strength analysis

Exemplary results of reduced stresses σ_{eq} [Pa] according to the hypothesis Huber-Misses-Hencky for selected angles ($\alpha = 0^o$ and $\alpha = 90^o$) operating of TPO shaft power transmission shown in figure 6 and 7.

Source: / Źródło:

Fig. 6. State of equivalent stresses in the jointed-telescopic shaft for angles of deviation in deriving and derived shafts $\alpha = 0^o$ (a) and $\alpha = 90^o$ (b)

Rys. 6. Stan naprężeń zredukowanych w wałku przegubowo-teleskopowym dla kątów odchylenia osi wału napędzającego i napędzanego $\alpha = 0^o$ (a) i $\alpha = 90^o$ (b)

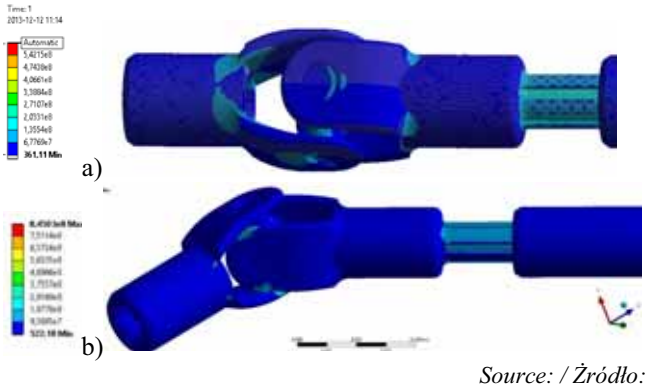

Source: / Źródło:

Fig. 7. State of equivalent stresses in the place of their maximum value concentration in jointed-telescopic for angles of axis deviation in deriving and derived shafts $\alpha = 0^o$ (a) and $\alpha = 90^o$ (b)

Rys. 7. Stan naprężeń zredukowanych w miejscach koncentracji ich maksymalnych wartości w wałku przegubowo-teleskopowym dla kątów odchylenia osi wału napędzającego i napędzanego $\alpha = 0^o$ (a) i $\alpha = 90^o$ (b)

Source: / Źródło:

Fig. 4. Solid model of jointed-telescopic Power Take-Off shaft with Cardan joint

Rys. 4. Model bryłowy wałka przegubowo-teleskopowego z przegubem Cardana

2.3. Fatigue wear analysis

The aim of the analysis was to determine the number of fatigue cycles work properly jointed-telescopic shaft, for the case of unilateral pulsating loads and different angles axis deviation for in deriving and derived shafts. The results of numerical calculations for angles in the range $\alpha = 0^o \div 90^o$ are shown graphical in figure 8. Also developed dependence of the number of cycles N the correct operation from the angle α in the form a polynomial of the second degree:

$$N = 3{,}2 \cdot \alpha^2 - 1182 \cdot \alpha + 95875, \qquad R = 0{,}9577. \qquad (1)$$

The analysis shows that the deviation angle α has a very significant influence on the fatigue strength of the shaft. For example, for an angle $\alpha = 0^o$ for fatigue strength are 98819 cycles (fig. 9a), while for an angle of $\alpha = 90^o$ is 15 750 cycles (fig. 9b), which is six times less.

Moreover, the fatigue curves are developed for various angles deviation α and torsion loads of the shaft in the range $M_o = 373 \div 1125$ [Nm]. For example, a load change in the range of 375 to 563 [Nm], an angle $\alpha = 0^o$ (Fig. 10a), causes a more than 130-fold decrease of fatigue strength, i.e. from cycle $N = 1{,}65 \cdot 10^7$ to $N = 1{,}25 \cdot 10^5$ cycle.

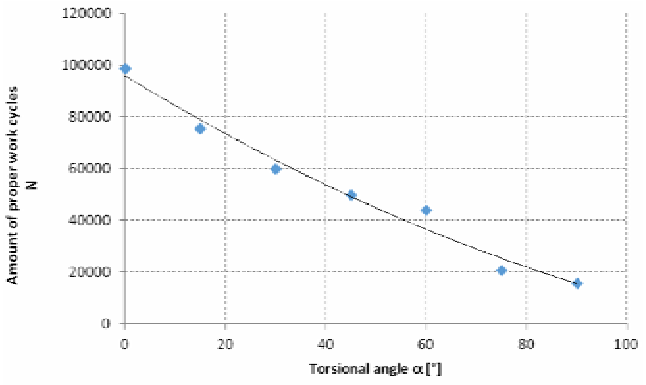

Source: / Źródło:

Fig. 8. Changing of the number of the correct cycles operation of the PTO shaft depending on the torsional angle
Rys. 8. Zmiana liczby cykli poprawnej pracy wałka przekaźnika mocy w zależności od kąta odchylenia

Source: / Źródło:

Fig. 9. Amount N of correct cycles of proper operation of the PTO shafts for the case of pulsating positive loads for various values of angle $\alpha = 0^o$ (a) and $\alpha = 90^o$ (b)
Rys. 9. Liczba cykli N poprawnej pracy dla przypadku obciążeń odwzorowano tętniących dodatnich dla różnych kątów odchylenia $\alpha = 0^o$ (a) i $\alpha = 90^o$ (b)

On the other hand increasing angle to $\alpha = 90^o$ results in a further nearly 10-fold reduction in the cycles from $N = 1{,}2 \cdot 10^6$ to $N = 2{,}5 \cdot 10^4$ (fig. 10b).

In addition, it is preferable to perform the modal calculation in order to determine the frequency and the shapes of free vibration also the harmonics calculation. This is necessary in case of a rigid connection of transmission drive components. Modal and harmonic calculations are performed for parts of machines, which during their life cycles are loaded, mainly rotational parts. These analyzes are designed to, at first to determine the values of free vibrations of a part (modal analysis) and then is necessary to check that, the part isn't in resonance frequencies, and then to determine the change in the displacements value, strains and stresses under the influence of variable frequency load operated part or assembly parts. These calculations were also performed for the shaft, showing the possibility of the developed application, and in order to check whether the rotational speed of the shaft doesn't work on the resonance frequency.

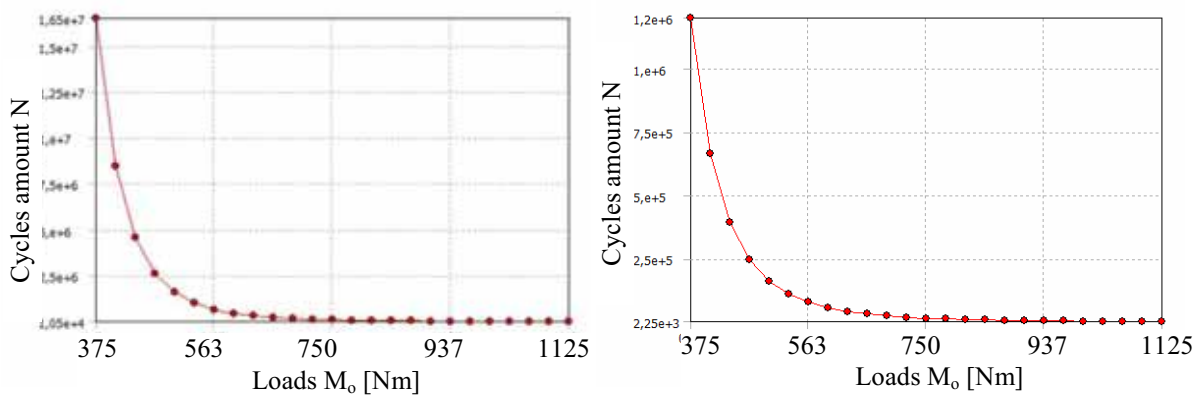

Source: / Źródło:

Fig. 10. The fatigue curves for different load moments Mo, for various values of angle $\alpha = 0^o$ (a) and $\alpha = 90^o$ (b)
Rys. 10. Krzywe zużycia zmęczeniowego dla różnych momentów obciążenia Mo, dla kątów odchylenia $\alpha = 0^o$ (a) i $\alpha = 90^o$ (b)

3. Modal and harmonic analysis

Analysis was carried out using FEM In this method, a construction model is a discrete system with a finite number of degrees of freedom. It is known that the differential equation describing the vibrations of a discrete system with N degrees of freedom can be represented in matrix form as [6, 7, 8]:

$$\mathbf{M}_{N\times N}\cdot\ddot{\mathbf{q}}_{N\times 1}+\mathbf{C}_{N\times N}\cdot\dot{\mathbf{q}}_{N\times 1}+\mathbf{K}_{N\times N}\cdot\mathbf{q}_{N\times 1}=\mathbf{F}(t)_{N\times 1}, \quad (2)$$

where **q** is the vector of degrees of freedom of the system, **F**(t) is a vector of external forces, and **M**, **C**, **K** are respectively called a mass (or inertia), damping and stiffness matrices.

Equation (2) is called the equation of motion, is in fact a system of N ordinary differential equations of the second order. These equations are coupled, if the matrices **M**, **C** and **K** aren't diagonal matrices. If the vector **F**(t) is equal to zero, then we are dealing with free vibration – without external loads. If in addition in the construction isn't dumping, it's free vibration.

The differential equation a free vibration of the discrete system can be written as:

$$\mathbf{M}\cdot\ddot{\mathbf{q}}+\mathbf{K}\cdot\mathbf{q}=0. \quad (3)$$

The general solution of this equation takes the following form:

$$\mathbf{q}(t)=\mathbf{q}_A\cos\omega t+\mathbf{q}_B\sin\omega t, \quad (4)$$

where: $\mathbf{q}_A$ and $\mathbf{q}_B$ are vector of constant.

The second derivative of the displacement vector is:

$$\ddot{\mathbf{q}}(t)=-\omega^2\mathbf{q}_A\cos\omega t+\omega^2\mathbf{q}_B\sin\omega t=-\omega^2\mathbf{q}. \quad (5)$$

Substituting (4) and (5) to (3) are obtained:

$$-\omega^2\mathbf{M}\mathbf{q}+\mathbf{K}\mathbf{q}=0, \quad (6)$$

and than:

$$(\mathbf{K}-\omega^2\mathbf{M})\mathbf{q}=0. \quad (7)$$

Equation (7) is called an own generalized equation. By a simple transformation can be reduced to the standard own problem $\mathbf{A}\mathbf{q}=\lambda\mathbf{q}$.

Equation (7) is a homogeneous linear system of equations whose solution, is simple, and solution is **q**=0. This system may, however, have other solutions if the matrix is $(\mathbf{K}-\omega^2\mathbf{M})$ singular matrix, than:

$$\det(\mathbf{K}-\omega^2\mathbf{M})=0. \quad (8)$$

Equation (8) is a polynomial of the nth degree with regard to the variable ω^2. Looking for zeroes ω_i of this polynomial. The value ω_i is called the frequencies of free vibration, and the corresponding vectors $\mathbf{q_i}$ that satisfy the equation (7) for the value ω_i – eigenvectors.

The physical interpretation of each eigenvector $\mathbf{q_i}$ represents the so-called self-form of free vibration for frequencies ω_i – is the displacements vectors, which describe the deformation of the construction, characteristic for this part of the vibration. The solution of equation (8) doesn't contain information about the amplitude of vibration. If the vector $\mathbf{q_i}$ is the solution (8), is also solution of $\mathbf{rq_i}$, where **r** – is any multiplier, is their solution. In practice, the eigenvectors are often presented after normalization into the relation to the mass matrix:

$$\mathbf{q}_i^T\mathbf{M}\mathbf{q}_i=1, \quad (9)$$

which makes to the corresponding scaling of the vector $\mathbf{q_i}$ coefficients. Knowing vector $\mathbf{q_i}$ defines the shape of the deformation of the model by a frequency vibration ω_i, which can also appoint suitable for the normalized frequency distributions of stresses.

In practice, an analysis of free vibrations it is necessary to analyse the presence of the resonance in elastic structures. The task of the designer is to design elastic properties or inertia to the frequency of free vibrations of the structure doesn't cover with the frequencies of typical external influences [6, 7, 8].

The calculation results of the frequency of free vibration of the shaft are shown in table 1.

Table 1. The calculation results of the frequency of free vibrations and their state

Tab. 1. Wyniki obliczeń częstotliwości drgań własnych i ich postaci

No of state of free vibration	The frequency of free vibration fw [Hz]	State of vibration
1	22,34	flexural
2	22,49	flexural
3	151,26	flexural
4	152,11	flexural
5	390,43	flexural
6	393,73	flexural

Source: / Źródło:

The chart shows that the shaft speed of $N=1000$ rpm frequency force is equal $f=16{,}7$ [Hz], which is lower than the first frequency of free vibration, so there is no danger of falling into the mechanical resonance.

The purpose of the harmonic analysis was to determine the changes of displacements, strains and stresses occurring in the shafts under the influence of variable of cyclic load changes. Numerical analyses were carried out by means of a Finite Element Method. Exemplary results of the calculations are shown in figure 11, which shows the increase normal stress in a plane perpendicular to the axis of the shaft with increases of the free vibration frequency, for the load moment $M_o=750$ [Nm]. Visible is a sharp decline in growth stresses beyond the first resonance frequency.

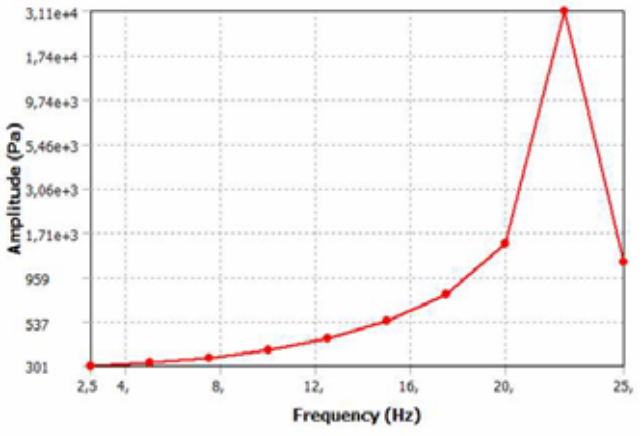

Source: / Źródło:

Fig. 11. Chart of dependence of normal stresses increase in a plane perpendicular to the axis of the shaft among with increases of the free vibration frequency

Rys. 11. Wykres zależności przyrostu naprężeń normalnych w płaszczyźnie prostopadłej do osi wału wraz ze wzrostem częstotliwości drgań

Exemplary solution results for equivalent stress for frequency 25 Hz and loads $M_o = 750$ is shown on figure 12.

Source: / Źródło:

Fig. 12. Map of increment of equivalent stresses σ_{eq} [MPa] of the shaft with the vibration frequency 25 Hz and a moment load $M_o = 750$ Nm

Rys. 12. Mapa przyrostu naprężeń zredukowanych σ_{eq} [MPa] w wale przy częstotliwości drgań 25 Hz i obciążeniu momentem $M_o = 750$ Nm

4. Conclusions

On the basis of numerical analysis and experimental research the following conclusions can be drawn:

1. Improper operation of jointed-telescopic shaft (eg. no turning off on the headland) leads to their premature fatigue wear.

2. Developed applications in the system ANSYS enables complex strength, modal, fatigue and harmonic analysis of jointed-telescopic power take-off shaft.

3. Conducted analysis let for determination of stress concentration. For the analyzed case demonstrates that the greatest equivalent stresses are in the same place, where occurring defects in fact.

4. Developed the fatigue wear curve, on based which we can predict the durability of the shaft, depending on the load moment and angle deviation for driving and driven shafts.

5. From numerical analysis of process it follows that the numerically tested system can withstand the load associated with the vibration phenomena and is a properly designed. Furthermore, it was found that the shaft at the maximum rotational operating speeds, is working at frequencies under resonance.

6. The developed application can be used also in the process of designing new jointed-telescopic shaft, in order to make complex analysis. At the first step it is possible to perform calculations of strength, fatigue, modal and harmonics. On the other hand, in the second stage, before production of designed shafts, is perform optimization (optimization of topological and parametric optimization [6, 11, 12]).

5. References

[1] Buch A.: Zagadnienia wytrzymałości zmęczeniowej. PWN, Warszawa 1964.
[2] Dacko M., Borkowski W., Dobrociński S., Niezgoda T., Wieczorek M.: Metoda Elementów Skończonych w mechanice konstrukcji. Arkady, Warszawa 1994.
[3] Gadomski W., Mróz S.: Ciągniki rolnicze. WSiP, Warszawa 1983.
[4] Hebda M., Wachal A.: Trybologia. WNT, Warszawa 1980.
[5] Kleiber M.: Wykłady z nieliniowej termo-mechaniki ciał odkształcalnych. Politechnika Warszawska, Warszawa 2000.
[6] Kukiełka L, Patyk R.: Nowoczesna metodyka projektowania części samochodowych. Ekologiczne aspekty stosowania nowych technologii w transporcie. Monografia. Politechnika Koszalińska, 2012, 215-246.
[7] Kułakowska A., Patyk R.: Numeryczna analiza drgań układu korbowo-tłokowego. Autobusy - technika, eksploatacja, systemy transportowe, 2011, 5, 329-333.
[8] Kułakowska A., Patyk R.: Topologiczna optymalizacja konstrukcji na przykładzie widłaka wału przegubowego. Autobusy, 2012, 5, 377-380. ISSN 1509-5878.
[9] Kutyłowski R.: Optymalizacja topologii kontinuum materialnego. Oficyna Wydawnicza Politechniki Wrocławskiej, Wrocław 2004.
[10] Łaczek S.: Wprowadzenie do systemu elementów skończonych ANSYS. PK, Kraków 1999.
[11] Szczepaniak J., Spadło M. 2012. Problematyka szacowania trwałości zmęczeniowej w projektowaniu maszyn rolniczych na przykładzie kombajnu do melioracji rowów. Inżynieria Rolnicza, Nr 4 (139), s. 411-420.
[12] Rakowski G., Kacprzak Z.: MES w mechanice konstrukcji. Oficyna Wydawnicza Politechniki Warszawskiej, Warszawa 2005.
[13] Rusiński E., Czmochowski J., Smolnicki T.: Zaawansowana metoda elementów skończonych w konstrukcji nośnych. Oficyna Wydawnicza Politechniki Wrocławskiej, Wrocław 2000.
[14] Towpik T.: Jak wybrać właściwie obroty wałka odbioru mocy ciągnika. Rolniczy przegląd Techniczny, 2004, 1.